

DYNAMIC BEHAVIOR OF PROPAGATING BUCKLES IN DEEP-WATER PIPELINE

The University of Tokyo, Member, Ha-Won Song

1. INTRODUCTION: At pressure higher than the propagation pressure in a deep-water pipeline, buckles can propagate along a pipeline at high speeds. This paper deals with dynamic buckle propagation under such pressure. For propagation under constant external pressure, it has been shown that the buckles advance at a constant speed known as the *propagation speed* [1,3].

Due to the high speed of the propagating buckles, it is evident that a propagating buckle can damage a substantial length of pipeline and result in great economic loss. Accordingly, the buckle arrestor has been devised to limit the length of damaged pipe. The buckle arrestor is a segment of pipe which is stronger than the main pipe and requires additional energy to plastically deform and flatten it (see fig. 1).

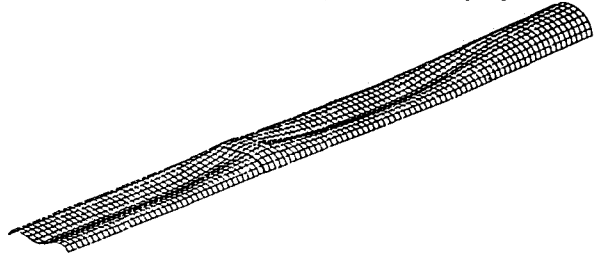


Fig. 1. Deformed Configuration of Pipe with an Arrestor.

Experimental results show that the efficiency of an arrestor is dependent on the dynamics of the problem and, in particular, on the conditions under which the propagating buckle engages the arrestor. Thus, it is imperative to investigate the dynamics of the propagating buckle in order to adequately and economically design buckle arrestors for pipelines, especially in deep water.

A finite element technique has been implemented, for the dynamic behavior of a pipe propagating at different pressures, by making use of nine-node isoparametric shell elements and considering the nonlinearities due to large deformation, elastoplastic material behavior and contact. Step-by-step integration in time has been carried out using the constant average acceleration method. As the pressure at which the buckle is initiated approaches the collapse pressure of the pipe, a different mode of buckle propagation is obtained and referred to as a *double propagating buckle*.

2. TECHNIQUE: The finite element employed in this work is based on the nine-node degenerated shell element. The formulation for the initial-boundary value problem described here uses an updated Lagrangian formulation of the field equations with a net of convected coordinates lines embedded and deforming with the body.

Material points are identified by a set of convected coordinates ξ^i . The kinematics of deformation of a body can be described by the three configurations indicated in fig. 2, namely,

1. reference configuration (*capital letter*) X at time t ,
2. current, deformed configuration (*small letter*) x at $(i - 1)$ th iteration of time $t + \Delta t$, and
3. nearby configuration (*small letter with a prime*) x' at (i) th iteration of time $t + \Delta t$.

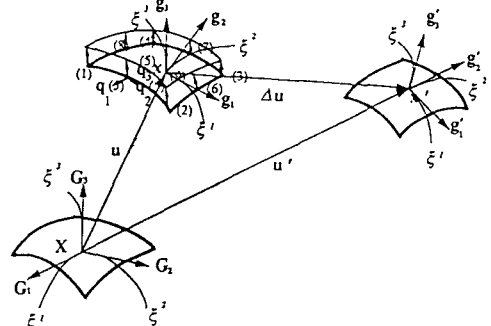


Fig.2. Kinematics and a Finite Element

An incremental equations of motion are obtained by applying the principle of virtual work to the two neighboring configurations X (with velocity \mathbf{V} and acceleration \mathbf{A}) and x' . The nonlinear incremental equation of motion at a nearby configuration x' , approximated using the constant average acceleration algorithm can be rewritten as:

$$\begin{aligned}
 & \frac{4}{\Delta t^2} \int_V \rho_{Ref} \delta \mathbf{u} \cdot \Delta \mathbf{u} \, dV + \int_V \delta U_{k,j} (\mathbf{G}^k \cdot \mathbf{g}'_j) \tau^{ij} \, dV \\
 &= \int_{b'} \delta \mathbf{u} \cdot \mathbf{t}' \, db' \\
 &- \frac{4}{\Delta t^2} \int_V \rho_{Ref} \delta \mathbf{u} \cdot \mathbf{u} \, dV + \frac{4}{\Delta t} \int_V \rho_{Ref} \delta \mathbf{u} \cdot \mathbf{V} \, dV + \int_V \rho_{Ref} \delta \mathbf{u} \cdot \mathbf{A} \, dV
 \end{aligned} \tag{1}$$

in which ρ_{Ref} is mass density, $\mathbf{G}^k(\mathbf{g}_i)$ is contravariant (covariant) base vectors, τ^{ij} is Kirchhoff stress tensor, and t^i is defined as tractions. In (1), $\Delta \mathbf{u} = \mathbf{x}' - \mathbf{x}$ and $\mathbf{u} = \mathbf{x} - \mathbf{X}$, i.e., $\Delta \mathbf{u}$ is the increment of displacement given by

$$\Delta \mathbf{u}(\xi^1, \xi^2, \xi^3) = \sum_{k=1}^9 \left[(\Delta \mathbf{u}^{(k)} - \Delta \theta_1^{(k)} \xi^3 \mathbf{q}_2^{(k)} + \Delta \theta_2^{(k)} \xi^3 \mathbf{q}_1^{(k)}) N^{(k)}(\xi^1, \xi^2) \right], \quad (2)$$

where $\Delta \mathbf{u}^{(k)}$ (three components), $\Delta \theta_1^{(k)}$, $\Delta \theta_2^{(k)}$, $k = 1, \dots, 9$, are the nodal displacements and rotations and $N^{(k)}$ are the shape functions. Associated with each node in fig. 2 are mutually orthogonal vectors, identified by $\mathbf{q}_1^{(k)}$, $\mathbf{q}_2^{(k)}$, and $\mathbf{q}_3^{(k)}$. The magnitude of $\mathbf{q}_3^{(k)}$, which is extending to the opposite surface of the element, is taken equal to the thickness of the shell. Nine nodes of the element have been located on one of the surfaces of the shell for the convenience of applying constraints due to contact of the internal surface of the shell. During buckle propagation in pipes, contact occurs between regions of the interior wall. The contact element is implemented based on the penalty formulation, i.e. if an integration point is found to penetrate, the stiffness of a fictitious linear spring is added into element stiffness. Based on J_2 -flow theory of plasticity with isotropic hardening, the elastoplastic constitutive equations relating the Jaumann rate of Kirchhoff stress to the stretching tensor are considered in this work.

3. RESULTS: Results are presented for an aluminum-alloy (Al-6061-T6) pipe in which the dimensions and material properties are given [2]. The mass density of the pipe, denoted by ρ_{Ref} , is such that $\sqrt{\sigma_o/\rho_{Ref}} = 1,072 \text{ ft/sec}$. Under the assumption that pipe is in vacuum, the analysis was carried out with the levels of external pressure equal to 276 psi and 396 psi with a 24-diameter segment of pipe and 456 psi with a 34-diameter segment of pipe.

Deformed configurations of propagating buckles initiated at the pressures 276 psi and 396 psi are shown with one at 156.1 psi in fig. 3. It was shown that a buckle propagates quasistatically at external pressure 156.1 psi [1]. Examination of the buckles shown in fig. 3, i.e., buckles propagating along the pipe at higher speeds at higher external pressure, reveals marked differences from the quasistatic buckle propagation.

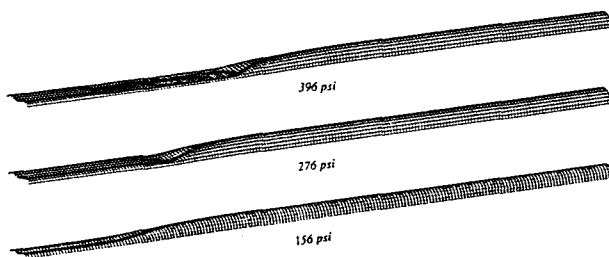


Fig.3 Propagating Buckles at Different Pressures

The buckle does steepen in the longitudinal direction as the pressure increases. The increase of steepness of the buckle as the pressure is raised from 156 psi to 396 psi is seen to be substantial. The cross sections at the tail of the propagating buckles at 396 psi are significantly flatter than the corresponding sections at 156 psi. Also, several instances of slight springback of the collapsed segment of the pipe can be identified. As the pressure at which the buckle is initiated approaches the collapse pressure of the pipe, 488 psi, a different mode of buckle propagation is obtained.

This mode can be referred to as a *double propagating buckle*. Successive deformed configurations of the pipe at pressure equal to 456 psi are shown in fig. 4.

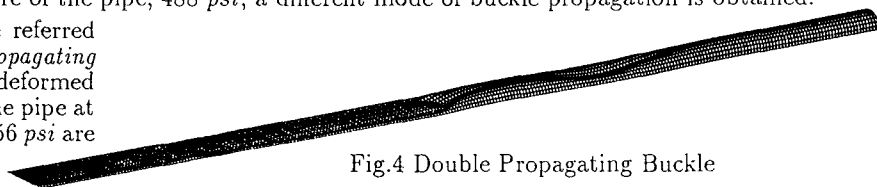


Fig.4 Double Propagating Buckle

It can be seen that as the buckle initiation process nears completion, the pipe in front of the collapsed segment undergoes substantial ovalization in the orthogonal direction so that the process of initiation of another buckle begins. Kyriakides and Babcock [1] observed similar flip-flop mode of buckle propagation in their experiments. Using the technique described here, the propagation speeds under different external pressure are obtained and are shown in [3].

4. REFERENCES:

- [1] Kyriakides, S., Babcock, C. D.; On the Dynamics and the Arrest of the Propagating Buckle in Off-shore Pipelines, Proceedings, Offshore Technology Conference, No. 3479, pp. 1035-1045, May 1979.
- [2] Song, H.-W.; Propagating Buckle Analysis of Deep-water Pipelines, Proceedings, 46th Annual Conference of JSCE, Osaka, Sept. 1991.
- [3] Song, H.-W., Tassoulas, J. L.; Dynamics of Propagating Buckles in Deep-Water Pipelines, Transactions Journal of Offshore Mechanics and Arctic Engineering, ASME., to appear.